IEEE Photonics Journal
An IEEE Photonics Society Publication

Open Access

All-Fiber OAM Amplifier With High Purity and Broadband Spectrum Gain Based on Fused Taper Vortex-Beam Coupler

Volume 6, Number 10, December 2018

Jianxiang Wen
Xinyu He
Jianfei Xing
Junfeng Yang
Fufei Pang
Xianglong Zeng
Zhenyi Chen
Tingyun Wang

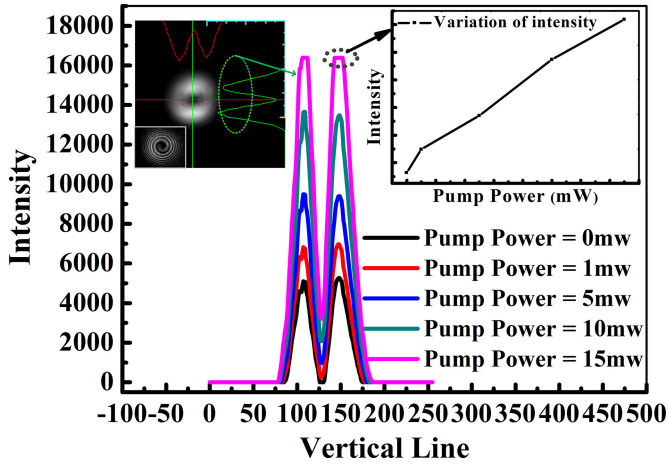

DOI: 10.1109/JPHOT.2018.2872040
1943-0655 © 2018 IEEE

All-Fiber OAM Amplifier With High Purity and Broadband Spectrum Gain Based on Fused Taper Vortex-Beam Coupler

Jianxiang Wen, Xinyu He, Jianfei Xing, Junfeng Yang, Fufei Pang, Xianglong Zeng, Zhenyi Chen, and Tingyun Wang

Key Laboratory of Specialty Fiber Optics and Optical Access Networks, Joint International Research Laboratory of Specialty Fiber Optics and Advanced Communication, Shanghai Institute for Advanced Communication and Data Science, Shanghai University, Shanghai 200444, China

DOI:10.1109/JPHOT.2018.2872040

Manuscript received July 19, 2018; revised September 18, 2018; accepted September 19, 2018. Date of publication October 18, 2018; date of current version October 24, 2018. This work was supported in part by the Natural Science Foundation of China under Grants 61520106014, 61475096, 61422507, and 61635006; and in part by the Science and Technology Commission of Shanghai Municipality, China under Grant 15220721500. Corresponding author: Jianxiang Wen (e-mail: wenjx@shu.edu.cn).
This paper has supplementary downloadable material available at http://ieeexplore.ieee.org.

Abstract: All-fiber orbital angular momentum (OAM) amplifier with high purity and broadband spectrum gain based on a fused taper vortex-beam coupler (VBC) has been studied. Active and passive few-mode fibers (FMFs), which have similar geometric parameters, are fabricated. A VBC using a single-mode fiber and a passive FMF is designed and fabricated. The VBC can generate the first-order OAM in the range of 1480–1640 nm and its purity up to 91%. Then, an all-fiber vortex amplification system is constructed for the first time, and the first-order OAM is amplified using this system with a low-gain difference ($\triangle$G). The gain exceeds 22 dB at 1549 nm, and its full width at half maximum is approximately 40 nm: 1519–1559 nm. This is a novel all-fiber OAM amplification system with a simple structure and low cost that is applicable in optical communication fields.

Index Terms: Optical vortices, optical amplifiers, fiber-optics amplifiers and oscillators.

1. Introduction

Vortex beams, which are also called orbital angular momentum (OAM) beams and carry an OAM of $l\hbar$ per photon, are a popular research topic in the field of communications. Vortex beams have a helical phase front that can be expressed as $\mathbf{e}^{il\theta}$, where l is the topological charge, and θ is the azimuthal angle. Thus, OAM beams have attracted considerable attention in the fields of special optical fibers and photo-communications. OAM beams have seen diverse applications, such as optical tweezers [1], atom manipulation [2], high-precision microscopy [3], information encoding and decoding [4], and optical communication [5]. A variety of methods for generating OAM beams have been proposed, including spatial light modulators [6], spiral phase plates [7], computer-generated holograms [8], cylindrical lens pairs [9], q-plates [10], fiber gratings [11], offset splicing technology [12], and couplers. The coupler was recently reported by S. Pidishety *et al.* [13]; however, it has high insertion loss of approximately 6 dB and can only generate OAM beams over a spectral range of 1 nm. In addition, the purity [14], transmission [15]—[17], and amplification of OAM beams

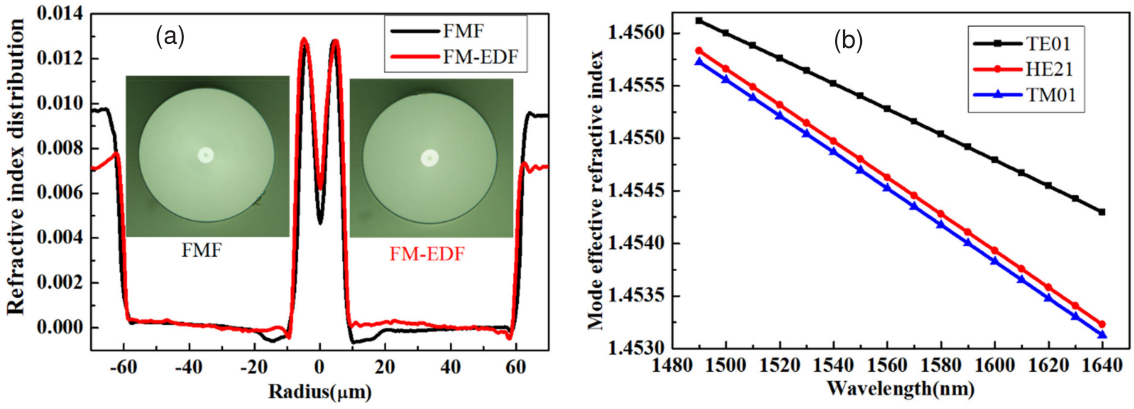

Fig. 1. (a) Refractive index distribution of FMF and FM-EDF; (b) Variation of mode effective refractive index with the increasing of wavelength in FMF.

have inspired the interest of researchers, who consider that OAM beams are more suitable to be information carriers than the linear-polarization (LP) mode. This is because OAM beams have lower crosstalk between adjacent modes and can be transmitted steadily in longer fibers [18]. Recently, research on mode amplification has mainly focused on the LP mode [19]–[24]. For example, a few-mode multi-element fiber amplifier and a gain-equalized few-mode erbium-doped fiber amplifier were reported. Y. Jung *et al.* reported the amplification of OAM, obtaining the gain of the first-order OAM according to an air–hole erbium-doped fiber [25]. However, these are not all-fiber OAM amplification systems.

In this study, we design and fabricate two kinds of few-mode fibers (FMFs), which are used to fabricate a vortex-beam coupler (VBC) with higher performance to generate and amplify the first-order OAM. Then, we construct an all-fiber OAM amplification system and realize a high purity and broadband amplification of the first-order OAM with a low gain difference (△G).

2. Fabrication of Optical Fiber

Two kinds of fibers, the passive FMF and active few-mode erbium doped fiber (FM-EDF), are designed and fabricated. FM-EDF is fabricated combining modified chemical vapor deposition (MCVD) with liquid solution methods [26], process is consisted of four parts. For the first step, a core layer should be obtained at lower temperature with conventional MCVD, which is partially sintered, opaque and porous. Then, the second step is to add the erbium ion in the core layer. Therefore, the tube with sediment core layer should be immersed in a solution containing erbium ion, and Erbium ion will be uniformly adsorbed in loose core layer after a while. Next, the tube with erbium ion is dried and dehydrated in an environment containing O_2, H_e and Cl_2. And then, the loose core layer is sintered and tube is melted condensation into a bar. Final step is to add a suitable annular tube based on diameter radio between cladding and core and preform. Geometry parameters of passive FMF are $D_{core} = 5\,\mu$m, $D_{ring} = 15\,\mu$m, $D_{cladding} = 125\,\mu$m. Geometry parameters of active FM-EDF are $D_{core} = 6\,\mu$m, $D_{ring} = 17.5\,\mu$m, $D_{cladding} = 125\,\mu$m, and they are of the similar geometry parameters, as shown in Fig. 1(a).Which results in OAM beams can transmit along the FMF and FM-EDF keeping the polarization state constant.

The refractive index profile is measured by optical fiber analyzer (S14, Photon Kinetics Inc., USA), as shown in Fig. 1(a). Refractive index differences of FMF and FM-EDF are both approximately 1.3%. It can be observed that the refractive index profile is a gradual step, and is of a double peak profile, which conforms to what we expect. According to geometry parameters, we simulate that mode effective refractive index difference (Δn_{eff}) between TE_{01} and HE_{21} is much more than 1×10^{-4}, as shown in Fig. 1(b). Which means that TE_{01}, HE_{21} and TM_{01} modes will not be degenerate. Therefore, $OAM_{\pm 1}$ only can be composed by HE_{21}^{even} and HE_{21}^{odd}, which indicates that $OAM_{\pm 1}$ can be

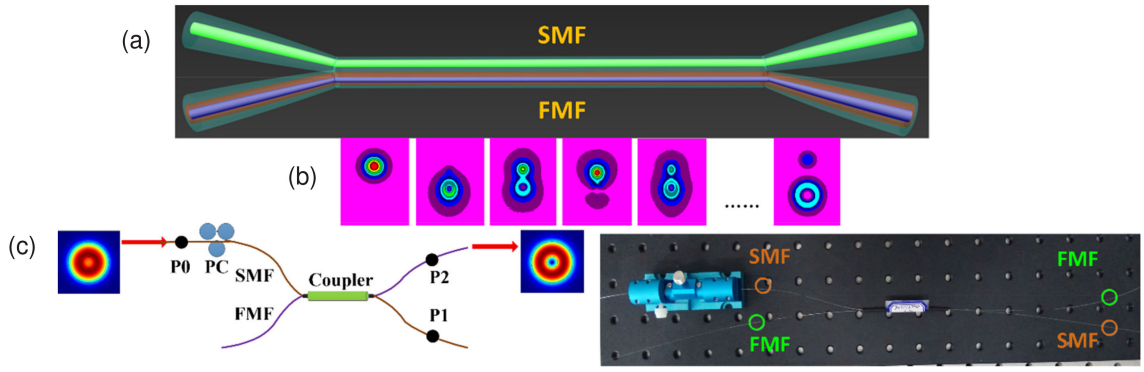

Fig. 2. (a) 3D simulation model of VBC; (b) Mode conversion process between HE_{11} in SMF and HE_{21} in FMF; (c) schematic diagram and sample of VBC.

transmitted steadily in the two kinds of fibers. To obtain high purity $OAM_{\pm 1}$ generated by VBC that is fabricated by SMF and FMF, all above are indispensable conditions. In addition, FM-EDF presents a very distinct feature that there exist strong absorptions, approximately 32.5 dB/m at 976 nm and 95 dB/m at 1535 nm, respectively, which can limit the mode coupling and background losses.

3. Generation of First-Order OAM

Here, we design and fabricate a kind of VBC, and then a high purity first order OAM can be generated. The principle of the VBC is closely following the coupling mode theory, in which the main process is that the HE_{11} mode in standard single-mode fiber (SMF) couples to HE_{21} or higher order vector mode in FMF. Coupling mode theory is a very suitable instrument that can analyze the coupling mechanism of fiber coupler thoroughly. The precondition of efficient coupling is the same mode effective refractive index (n_{eff}). Its content is that if the optical fiber coupling system only consists of two fibers, we can get the coupling model equation as:

$$\frac{dA_1(z)}{dz} + i\beta_1 A_1(z) = -ik_{12}A_2(z) \tag{1}$$

$$\frac{dA_2(z)}{dz} + i\beta_2 A_2(z) = -ik_{21}A_1(z) \tag{2}$$

Where A_1 and A_2 are the excited mode amplitudes in each fiber, respectively; β_1 and β_2 are the propagation constants of excited modes in two fibers, k_{12} and k_{21} are the coupling coefficients and $k_{12} \approx k_{21} = k$ which depends on the cross-section geometry and index profile of the fibers. We assumed $\beta_1 = \beta_2 = \beta$, which means the phase mismatch is zero, $a_1(z) = A_1(z)e^{j\beta_1 z}$, and $a_2(z) = A_2(z)e^{j\beta_2 z}$. After a detailed calculation and analysis, the status of power between two fibers can be expressed as:

$$P_1 = |a_1(z)|^2 = \cos^2(kz) \tag{3}$$

$$P_2 = |a_2(z)|^2 = \sin^2(kz) \tag{4}$$

Where P_1 and P_2 are the output power of SMF and FMF, respectively. From the equations above, we notice that the power present a complete periodic transfer and can be fully converted between two fibers when coupling length $L_c = \pi/2k$.

Based on the theoretical calculation above, we build up a 3D simulation model by utilizing beam propagation method with the commercial simulation software (RSoft). Here, SMF is the standard single-mode fiber (Corning SMF-28e), geometry of FMF includes core, ring and cladding layers, and the cladding is fused together at the coupling region, as shown in Fig. 2(a).When HE_{11} mode is injected in SMF, it begins to couple to HE_{21} mode in FMF during the beam propagation process.

Along with the increasing of transmission distance, firstly, HE_{11} is all converted to HE_{21} mode; secondly, HE_{21} is coupled to HE_{11} mode, a mode coupling cycle is completed. Cycle number of this coupling process is determined by the length of the coupler region, as shown in Fig. 2(b). Which shows that HE_{11} in SMF is efficiently coupled to HE_{21} in FMF.

According to the theoretical simulation above, we fabricate a VBC and setup an observation system. The production process of VBC is divided into four steps. Firstly, SMF is pre-stretched to designated size in order to match the size of FMF, which conforms to the phase-matching condition between HE_{11} in SMF and higher order mode in FMF. Secondly, pre-stretched SMF and FMF are twisted a circle in the middle of tapered region. Coupling radio is set at the moment and the stretching velocity is set to 100–150 μm/s, 50–80 μm/s and 10–30 μm/s before coupling, coupling start and adjustment, respectively. Then, two fibers that have been twisted are pulled to both sides with oxyhydrogen flame and the pulling length is from 7000 μm to 8000 μm. The coupling region is uniform. Its diameter (waist diameter) is from 40 μm to 60 μm and the length of coupling region is from 15000 μm to 20000 μm. Finally, the VBC is loaded and fixed in a groove of quartz by using ultraviolet curing adhesive and covered by a heat shrinkable tube as a protection.

When HE_{11} is injected from SMF, $OAM_{\pm 1}$ can be obtained at the output of FMF by the observation system. Furthermore, HE_{11} mode can be coupled to $OAM_{\pm 1}$ in C+L bands, which ranges from 1480 nm to 1640 nm. The schematic diagram and sample of VBC are shown in Fig. 2(c). P_0 is the input power of SMF, P_1 and P_2 are the output power of SMF and FMF, respectively. Here, HE_{11} mode coupling to $OAM_{\pm 1}$ can be completed by VBC, however, the simulation process cannot be shown in Fig. 2(b). The cause that OAM mode cannot be observed is that the polarization state of HE_{11} in SMF is unmodified at the software. Information of the VBC in details is shown below, its working wavelength is from 1480 nm to 1640 nm containing C+L bands. Conversion efficiency (CE), which equals to P_2/P_0, of VBC is up to 60.8% and average CE of $\sim$60% is achieved at 1550 nm. Coupling ratio (CR), which equals to $P_2/(P_1 + P_2)$, is up to 100% and average CR of $\sim$85% is achieved at 1550 nm. Excess loss (EL) is less than 1 dB. $OAM_{\pm 2}$ also can be generated, then it needs to be optimized.

4. Amplification and Feature Analysis of OAM

We setup an all-fiber OAM amplification system, which consists of VBC, FM-EDF and real-time monitoring system, as shown in Fig. 3(a). Wavelength of the tunable laser (Key sight 81600B) ranges from 1480 nm to 1640 nm; Effective spectrum of broadband light source (SL3215-1550) ranges from 1400 nm to 1700 nm; Output power of 980 nm laser is more than 1 W, which can provide sufficient pumping power for this system; Polarization controller (PC) is to adjust the polarization state of LP_{01} in the SMF; Optical spectrum analyzer (OSA, Yokogawa AQ-6315A) is to quantitatively measure the performance of amplification; Charge Coupled Device (CCD HAMAMATSU C10633) is to observe the change of transverse mode field intensity in real time; Dichroic mirror (DM) is to filter out unabsorbed pumping light with high reflection at 750 – 1100 nm and high transmission at 1260-1700 nm. VBC that we design and fabricate with our own FMF is used as mode converter. FM-EDF, whose geometry parameters are similar to that of FMF, is used as gain medium. The length of FM-EDF is 1.0 m. In addition, in this system, OAM beams can transmit along the FMF and FM-EDF keeping the polarization state constant, which benefits from the similar geometry parameters of FMF and FM-EDF.

Before the experiment, wavelength of signal light is fixed at 1550 nm, the power is 500 μW, and pumping power is set as 0 mW. Firstly, the signal light is turned on, HE_{11} mode couples to $OAM_{\pm 1}$ mode after the VBC. Secondly, $OAM_{\pm 1}$ transmits along FM-EDF, and its polarization state keeps constant. Thirdly, transverse mode field intensity of $OAM_{\pm 1}$ can be obtained at D, as shown in Fig. 3(b). The data of vertical line (green line) is extracted to analyze amplification performance. Fourthly, pumping power is turned on and changed from 1 mW to 15 mW. Along with the changing of pumping power, data of green line is recorded and integrated, as shown in Fig. 3(c). Horizontal axis represents the green line in Fig. 3(b), vertical axis represents intensity. This figure shows that the profile of transverse mode field keeps constant and the intensity of transverse mode field is

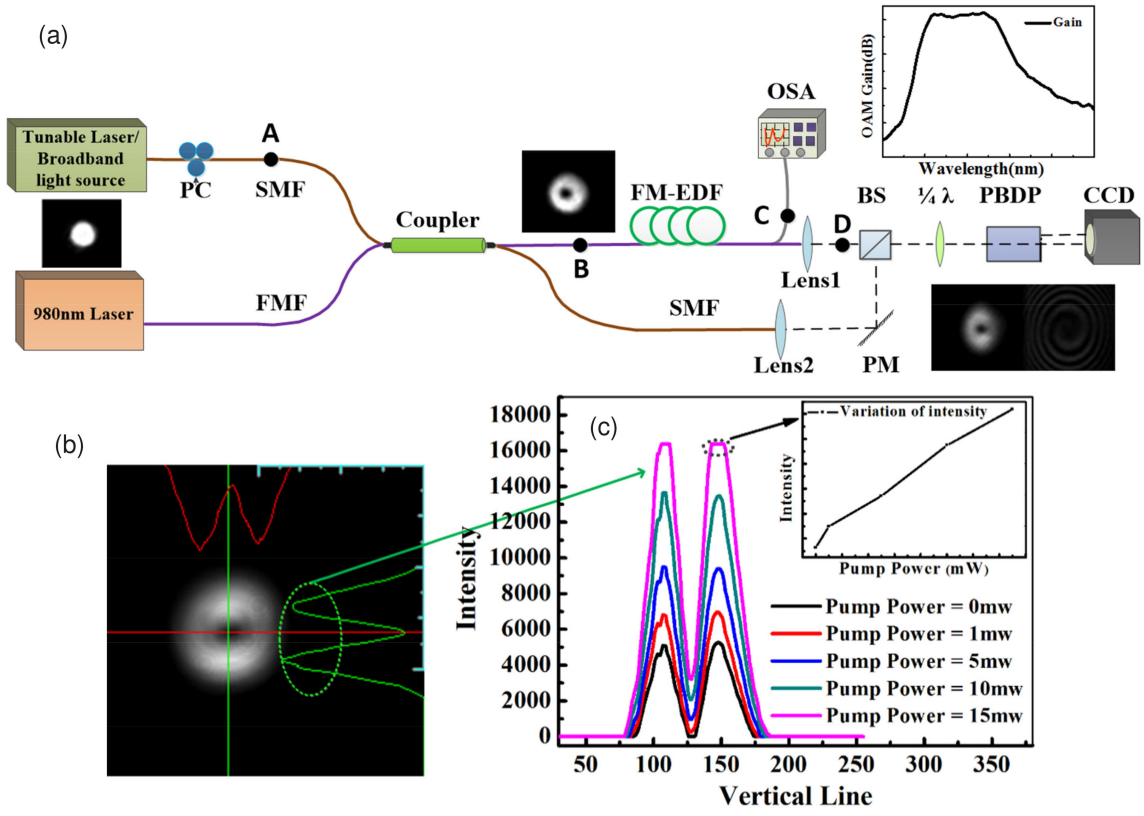

Fig. 3. (a) Schematic diagram of all-fiber vortex amplification system; (b) Transverse mode field intensity of first order OAM; (c) Variation of transverse mode field intensity with the increasing of pumping power.

increased with the increasing of pumping power, until intensity of CCD is up to saturation. These show that first order OAM has been amplified, as shown in Fig. 3(c).

To further illustrate the amplification of first order OAM, tunable laser is replaced by broadband light source as the signal light. Here, the length of FM-EDF is fixed at 1.0 m, the power of signal light and pump light are fixed at -20 dBm and 600 mW, respectively. All of the devices are turned on, spectra about this all-fiber OAM amplification system are recorded and integrated, as shown in Fig. 4(a). Blue line is signal light from broadband, black line is amplified spontaneous emission (ASE) of FM-EDF after injecting pumping power, and red line is the sum of pumping power and signal light. Pink line, which equals to difference between red and blue line, represents On-Off gain. Green line, which equals to red line that has been removed the power of signal light (blue line) and ASE (black line), represents net gain. Net gain spectrum is also shown in Fig. 4(b). It shows that the maximum gain value approximately 22 dB is obtained at 1549 nm, and 3 dB bandwidth is approximately 40 nm. The better flatness of gain spectrum from 1522 nm to 1553 nm (gain difference (ΔG) $<$ 1.1 dB) is obvious because of the special structure of FM-EDF. We can further optimize the distribution of erbium ion and refractive index in FM-EDF or change the modes of pumping (LP_{01}, LP_{11} *or* $OAM_{\pm 1}$) to improve gain effect. Here, mode of pumping is set as first order OAM, and the result shows that net gain is improved.

Then, we take out some point sites at different wavelengths (1520, 1550, 1570, and 1600 nm) from the spectrum, as shown in Fig. 4(b), and observe helical interference fringes of first order OAM before and after amplification. Here, broadband light source is replaced by tunable laser, which can get single-wavelength signal light, and their functions are identical. The experimental results show that first order OAM of signal light at different wavelengths have been amplified, respectively. This is an interesting phenomenon that the value of topological charge ℓ is same at different wavelengths of

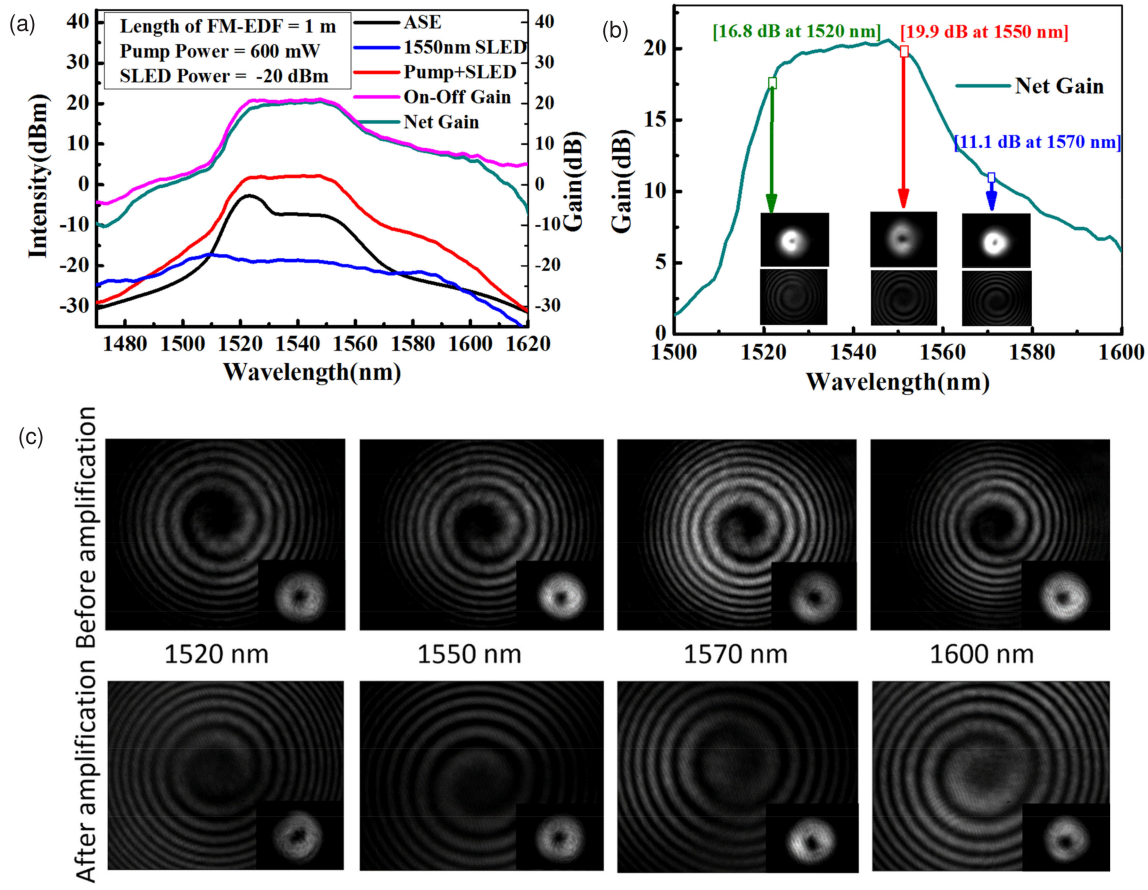

Fig. 4. (a) Spectra of all-fiber OAM amplification system in each node; (b) Net gain spectrum of first order OAM; (c) First and second row are helical interference fringes and transverse mode profiles of first order OAM before and after amplification, respectively.

C+L bands, which is corresponding to the performance of VBC before and after amplification, and the state of first order OAM remains stable. Furthermore, a length of FM-EDF is added in the system when first order OAM is amplified. Therefore, there is a slight difference about helical interference fringes before and after amplification, which caused by the different optical path difference (OPD), as shown in Fig. 4(c).

Purity is an important parameter to evaluate the quality of OAM beam. High purity OAM beam is the basis of vortex laser and vortex amplifier, and it is also the precondition of vortex optical communication system. Calculation method of first order OAM purity has been reported by N. Bozinovic, *et al.* [27], a vortex basis set is built up:

$$V_{11}^{+}(r,\theta) = \left(HE_{11}^{x} + iHE_{11}^{y}\right)/\sqrt{2} = (\hat{x} + i\hat{y})\,F_{01}(r)/\sqrt{2} \tag{5}$$

$$V_{11}^{-}(r,\theta) = \left(HE_{11}^{x} - iHE_{11}^{y}\right)/\sqrt{2} = (\hat{x} - i\hat{y})\,F_{01}(r)/\sqrt{2} \tag{6}$$

$$V_{21}^{+}(r,\theta) = \left(HE_{21}^{e} + iHE_{21}^{o}\right)/\sqrt{2} = e^{j\theta}(\hat{x} + i\hat{y})\,F_{11}(r)/\sqrt{2} \tag{7}$$

$$V_{21}^{-}(r,\theta) = \left(HE_{21}^{e} - iHE_{21}^{o}\right)/\sqrt{2} = e^{-i\theta}(\hat{x} - i\hat{y})\,F_{11}(r)/\sqrt{2} \tag{8}$$

$$V_{T}^{+}(r,\theta) = \left(TM_{01} - iTE_{01}\right)/\sqrt{2} = e^{-i\theta}(\hat{x} + i\hat{y})\,F_{11}(r)/\sqrt{2} \tag{9}$$

$$V_{T}^{-}(r,\theta) = \left(TM_{01} + iTE_{01}\right)/\sqrt{2} = e^{i\theta}(\hat{x} - i\hat{y})\,F_{11}(r)/\sqrt{2} \tag{10}$$

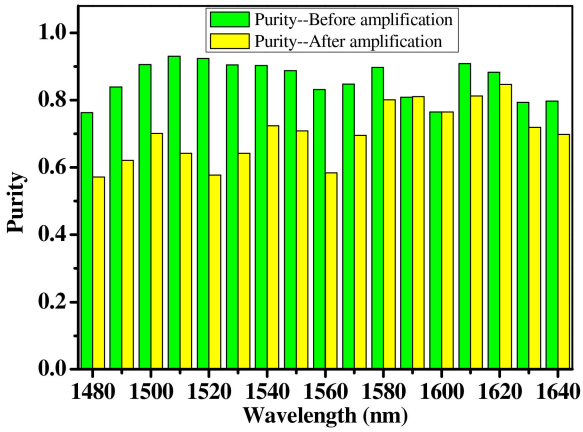

Fig. 5. Variation of purity with wavelength before and after amplification.

After a detailed and standard calculation and analysis, mode power contributions (purity) as:

$$MPI_l^s = 10\log_{10}\left(\left|\gamma_l^s\right|^2 / P_{tot}\right) \tag{11}$$

Where γ_l^s is the mode field complex amplitude of the vortex basis vectors, $P_{tot} = \sum_{l=(11,21,T)} \sum_{s=(+,-)} |\gamma_l^s|^2$. Based on this method, we calculate the purity of first order OAM before and after amplification. The purity of first order OAM, other than four sample points (@1480, 1600, 1630, 1640 nm), is up to 80%, and purity of six sample points are up to 90% before amplification. The average purity of first order OAM is up to 86% and 71% at different wavelengths from 1480 nm to 1640 nm before and after amplification, respectively. And the difference of purity is small between different wavelengths. However, there is a phenomenon that the purity of first order OAM is different before and after amplification. And the difference value is bigger at range of 1480–1580 nm than other wavelengths, which reason is that this range is the erbium ion absorption band. Furthermore, the purity before amplification is better than after amplification, and the reason for that is the absorption of erbium ion and geometry of FM-EDF, as shown in Fig. 5.

5. Conclusion

We design and fabricate two kinds of FMFs with similar geometry parameters, a passive FMF, which is used to fabricate VBC together with SMF, and an active FM-EDF, which is used to amplify OAM beam generated by VBC. And the VBC can generate first order OAM at the range of C+L bands. Then, we setup an all-fiber OAM amplification system, and obtain the maximum gain approximately 22 dB at 1549 nm. The FWHM of this all-fiber OAM amplification system is approximately 40 nm, and gain spectrum from 1522 nm to 1553 nm is flatness ($\Delta G < 1.1$ dB). The purity of first order OAM is up to 93% at 1510 nm, and average purity is up to 86% and 71% at different wavelengths from 1480 nm to 1640 nm before and after amplification, respectively. This all-fiber amplification system can be applied in vortex beams laser and optical amplifier in vortex transmission system. Next, we will further optimize the geometry parameters of FMF and FM-EDF to match better together for OAM beam, and investigate the higher order OAM optical amplification system.

References

[1] M. Padgett and R. Bowman, "Tweezers with a twist," *Nat. Photon.*, vol. 5, no. 6, pp. 343–348, 2011.
[2] H. Kawauchi, K. Yonezawa, Y. Kozawa, and S. Sato, "Calculation of optical trapping forces on a dielectric sphere in the ray optics regime produced by a radially polarized laser beam," *Opt. Lett.*, vol. 32, no. 13, pp. 1839–1841, 2007.

[3] O. J. Allegre, W. Perrie, S. P. Edwardson, G. Dearden, and K. G. Watkins, "Laser microprocessing of steel with radially and azimuthally polarized femtosecond vortex pulses," *J. Opt.*, vol. 14, no. 8, 2012, Art. no. 085601.
[4] L. C. Crasovan, G. Molina-Terriza, J. P. Torres, L. Torner, V. M. Pérez-García, and D. Mihalache, "Globally linked vortex clusters in trapped wave fields," *Phys. Rev. E*, vol. 66, no. 3, 2002, Art. no. 036612.
[5] N. Bozinovic *et al.*, "Terabit-scale orbital angular momentum mode division multiplexing in fibers," *Science*, vol. 340, no. 6140, pp. 1545–1548, 2013.
[6] A. Cofré, P. García-Martínez, A. Vargas, and I. Moreno, "Vortex beam generation and other advanced optics experiments reproduced with a twisted-nematic liquid-crystal display with limited phase modulation," *Eur. J. Phys.*, vol. 38, no. 1, 2016, Art. no. 014005.
[7] M. W. Beijersbergen, R. P. C. Coerwinkel, M. Kristensen, and J. P. Woerdman, "Helical-wavefront laser beams produced with a spiral phaseplate," *Opt. Commun.*, vol. 112, no. 5/6, pp. 321–327, 1994.
[8] N. R. Heckenberg, R. McDuff, C. P. Smith, and A. G. White, "Generation of optical phase singularities by computer-generated holograms," *Opt. Lett.*, vol. 17, no. 3, pp. 221–223, 1992.
[9] M. W. Beijersbergen, L. Allen, H. E. L. O. Van der Veen, and J. P. Woerdman, "Astigmatic laser mode converters and transfer of orbital angular momentum," *Opt. Commun.*, vol. 96, no. 1/3, pp. 123–132, 1993.
[10] L. Marrucci *et al.*, "Spin-to-orbital conversion of the angular momentum of light and its classical and quantum applications," *J. Opt.*, vol. 13, no. 6, 2011, Art. no. 064001.
[11] Y. Zhao, Y. Liu, L. Zhang, C. Zhang, J. Wen, and T. Wang, "Mode converter based on the long-period fiber gratings written in the two-mode fiber," *Opt. Exp.*, vol. 24, no. 6, pp. 6186–6195, 2016.
[12] X. Jin *et al.*, "Generation of the first-order OAM modes in single-ring fibers by offset splicing technology," *IEEE Photon. Technol. Lett.*, vol. 28, no. 14, pp. 1581–1584, Jul. 2016.
[13] S. Pidishety, S. Pachava, P. Gregg, S. Ramachandran, G. Brambilla, and B. Srinivasan, "Orbital angular momentum beam excitation using an all-fiber weakly fused mode selective coupler," *Opt. Lett.*, vol. 42, no. 21, pp. 4347–4350, 2017.
[14] N. Bozinovic, S. Golowich, P. Kristensen, and S. Ramachandran, "Control of orbital angular momentum of light with optical fibers," *Opt. Lett.*, vol. 37, no. 13, pp. 2451–2453, 2012.
[15] A. E. Willner *et al.*, "Optical communications using orbital angular momentum beams," *Adv. Opt. Photon.*, vol. 7, no. 1, pp. 66–106, 2015.
[16] B. Ung, P. Vaity, L. Wang, Y. Messaddeq, L. A. Rusch, and S. LaRochelle, "Few-mode fiber with inverse-parabolic graded-index profile for transmission of OAM-carrying modes," *Opt. Exp.*, vol. 22, no. 15, pp. 18044–18055, 2014.
[17] S. Ramachandran and P. Kristensen, "Optical vortices in fiber," *Nanophotonics*, vol. 2, no. 5/6, pp. 455–474, 2013.
[18] N. Bozinovic, P. Kristensen, and S. Ramachandran, "Long-range fiber-transmission of photons with orbital angular momentum," in *Proc. Int. Conf. Lasers Electro-Opt.*, 2011, Paper CTuB1.
[19] Y. Jung *et al.*, "First demonstration and detailed characterization of a multimode amplifier for space division multiplexed transmission systems," *Opt. Exp.*, vol. 19, no. 26, pp. B952–B957, 2011.
[20] G. Le Cocq *et al.*, "Modeling and characterization of a few-mode EDFA supporting four mode groups for mode division multiplexing," *Opt. Exp.*, vol. 20, no. 24, pp. 27051–27061, 2012.
[21] Y. Jung *et al.*, "Three mode Er 3+ ring-doped fiber amplifier for mode-division multiplexed transmission," *Opt. Exp.*, vol. 21, no. 8, pp. 10383–10392, 2013.
[22] Y. Jung *et al.*, "Cladding pumped few-mode EDFA for mode division multiplexed transmission," *Opt. Exp.*, vol. 22, no. 23, pp. 29008–29013, 2014.
[23] S. Jain, Y. Jung, T. C. May-Smith, S. U. Alam, J. K. Sahu, and D. J. Richardson, "Few-mode multi-element fiber amplifier for mode division multiplexing," *Opt. Exp.*, vol. 22, no. 23, pp. 29031–29036, 2014.
[24] Z. Zhang, Q. Mo, C. Guo, N. Zhao, C. Du, and X. Li, "Gain equalized four mode groups erbium doped fiber amplifier with LP 01 pump," in *Proc. Asia Conf. Commun. Photon.*, 2016, Paper ATh3B-5.
[25] Y. Jung *et al.*, "Optical orbital angular momentum amplifier based on an air-hole erbium-doped fiber," *J. Lightw. Technol.*, vol. 35, no. 3, pp. 430–436, Feb. 2017.
[26] A. S. Webb, A. J. Boyland, R. J. Standish, S. Yoo, J. K. Sahu, and D. N. Payne, "MCVD in-situ solution doping process for the fabrication of complex design large core rare-earth doped fibers," *J. Non-Cryst. Solids*, vol. 356, no. 18/19, pp. 848–851, 2010.
[27] N. Bozinovic, S. Golowich, P. Kristensen, and S. Ramachandran, "Control of orbital angular momentum of light with optical fibers," *Opt. Lett.*, vol. 37, no. 13, pp. 2451–2453, 2012.